

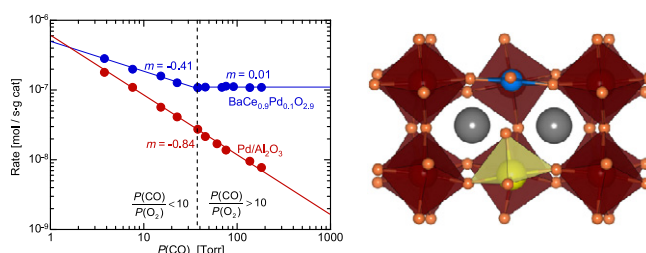


Contents

Mechanism for CO oxidation catalyzed by Pd-substituted BaCeO₃, and the local structure of the active sites

pp 83–91

Xiaoying Ouyang, Susannah L. Scott*

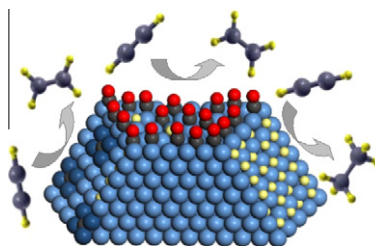


Low surface area, crystalline Ba(Ce,Pd)O₃ catalyzes CO oxidation using either oxygen adsorbed from the gas phase or labile lattice oxygen, and the rate law depends strongly on the $P(\text{CO})/P(\text{O}_2)$ ratio. Catalytic activity is attributed to the presence of square-planar Pd(II) ions located on the perovskite *B*-sites, each adjacent to an oxygen vacancy.

Interplay between carbon monoxide, hydrides, and carbides in selective alkyne hydrogenation on palladium

pp 92–102

Mónica García-Mota, Blaise Bridier, Javier Pérez-Ramírez*, Núria López**

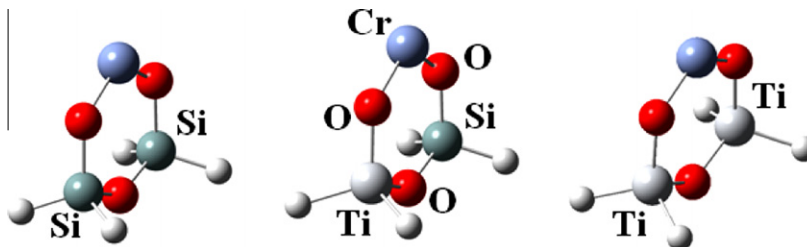


The selectivity of alkyne hydrogenation on Pd depends on the subsurface chemistry. CO blocks the dynamic state of the catalyst and turn it into a robust, selective configuration.

High-resolution spectroscopy (XPS, ¹H MAS solid-state NMR) and DFT investigations into Ti-modified Phillips CrO_x/SiO₂ catalysts

pp 103–115

Ruihua Cheng, Chen Xu, Zhen Liu, Qi Dong, Xuelian He, Yuwei Fang, Minoru Terano, Yatao Hu, Thomas J. Pullukat, Boping Liu*



DFT investigations combined with high-resolution XPS and ¹H MAS solid-state NMR characterization were carried out to elucidate the mechanism of Ti-modification on Phillips catalyst for ethylene polymerization.

Improved performance of TiO₂ in the selective photo-catalytic oxidation of cyclohexane by increasing the rate of desorption through surface silylation

pp 116–124

Ana Rita Almeida, Joana T. Carneiro, Jacob A. Moulijn, Guido Mul*

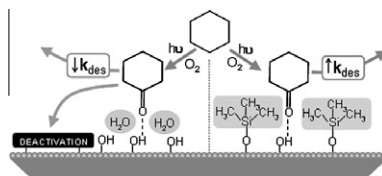
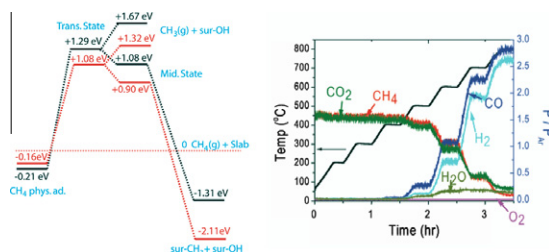


Photo-oxidation of cyclohexane over TiO₂ yields surface adsorbed Cyclohexanone. Desorption of this product is increased by silylation of the TiO₂ surface, reducing the rate of catalyst deactivation.

Methane complete and partial oxidation catalyzed by Pt-doped CeO₂

pp 125–137

Wei Tang, Zhenpeng Hu, Miaojun Wang, Galen D. Stucky, Horia Metiu*, Eric W. McFarland

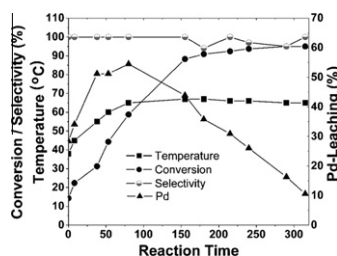


Energy level diagram (calculated) for breaking the C–H bond of methane. Steady state output from the reactor at different temperatures, for methane dry reforming. The catalyst is Pt-doped CeO₂.

Palladium leaching dependent on reaction parameters in Suzuki–Miyaura coupling reactions catalyzed by palladium supported on alumina under mild reaction conditions

pp 138–146

Saeeda S. Soomro, Farzana L. Ansari, Konstantinos Chatziapostolou, Klaus Köhler*

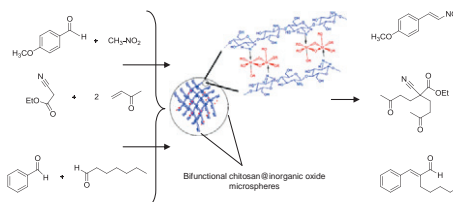


Various reaction parameters including temperature, solvent, base, substrates and additives influence the palladium leaching in Suzuki coupling reactions catalyzed by Pd/Al₂O₃. An efficient palladium dissolution–re-deposition process ensures high catalyst activity.

Decoration of chitosan microspheres with inorganic oxide clusters: Rational design of hierarchically porous, stable and cooperative acid–base nanoreactors

pp 147–155

Abdelkrim El Kadib*, Karine Molvinger, Mosto Bousmina, Daniel Brunel

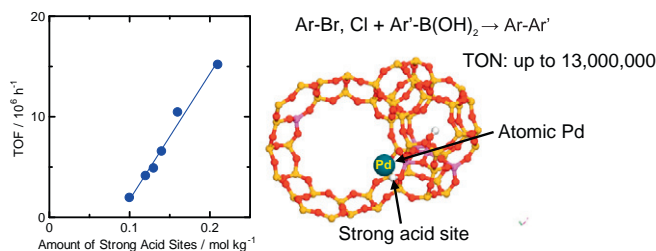


Mimicking enzyme action in solid materials: the cohabitation in close proximity of NH₂ from chitosan and acidic inorganic oxide in the replicated hybrid microsphere leads to cooperative action in catalysis.

Origin of the excellent catalytic activity of Pd loaded on ultra-stable Y zeolites in Suzuki–Miyaura reactions

pp 156–166

Kazu Okumura*, Takuya Tomiyama, Shizuyo Okuda, Hiroyuki Yoshida, Miki Niwa

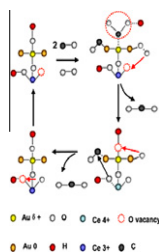


Pd loaded on USY zeolite exhibited very high activity in Suzuki–Miyaura reactions. The active species was proposed to be the atomic Pd anchored to the strong acid sites of USY.

Ultra-low-gold loading Au/CeO₂ catalysts for ambient temperature CO oxidation: Effect of preparation conditions on surface composition and activity

pp 167–176

Qiaoling Li, Yuanhua Zhang, Guoxing Chen, Jianqiang Fan, Hongqiao Lan*, Yiquan Yang**

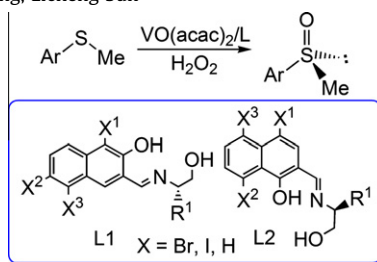


The Au⁰/Au⁺ ratio and the amount of water-derived species on the surface of Au/CeO₂ catalysts were found to be two important parameters affecting the activities.

Highly enantioselective sulfoxidation with vanadium catalysts of Schiff bases derived from bromo- and iodo-functionalized hydroxynaphthaldehydes

pp 177–181

Ying Wang, Mei Wang*, Yu Wang, Xiuna Wang, Lin Wang, Licheng Sun**

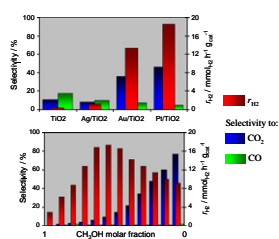


Chiral Schiff bases with a bromo- and iodo-functionalized naphthyl backbone proved to be efficient ligands for the vanadium-catalyzed asymmetric oxidation of aryl methyl sulfides in dichloromethane and toluene with up to 99% ee and moderate-to-high isolated yields.

Hydrogen production by photocatalytic steam reforming of methanol on noble metal-modified TiO₂

pp 182–190

Gian Luca Chiarello, Myriam H. Aguirre, Elena Selli*

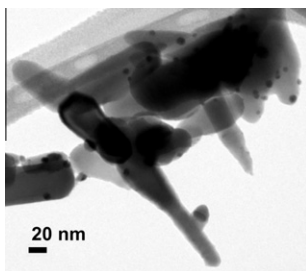


The rate of photocatalytic hydrogen production r_{H_2} from methanol/water vapours over noble metal (NB) – modified TiO₂ and the selectivity to different methanol oxidation products were found to correlate with the NB work function and with NB particles' size and dispersion. They sensibly varied with the H₂O/CH₃OH molar ratio in the gas-phase reactants mixture.

Catalytic performance of Au/ZnO nanocatalysts for CO oxidation

pp 191–198

S.A.C. Carabineiro*, B.F. Machado, R.R. Bacsá, P. Serp**, G. Dražić, J.L. Faria, J.L. Figueiredo

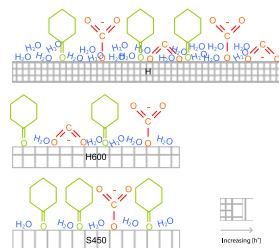


ZnO prepared by chemical vapour deposition with gold loaded by ultrasonication was very active for CO oxidation. The unique catalyst–substrate interaction (epitaxy related) might be related with the results observed.

Photocatalytic oxidation of cyclohexane by titanium dioxide: Catalyst deactivation and regeneration

pp 199–210

Joana T. Carneiro, Jacob A. Moulijn, Guido Mul*

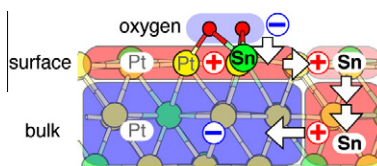


The catalyst stability in photocatalytic oxidation of cyclohexane and surface chemistry of TiO₂ are a strong function of the hydrophilicity of the surface and the crystal 'quality', affecting the concentration of reactive holes. Well-defined crystals with hydrophobic surfaces induce favorable catalyst properties.

Mediatory role of tin in the catalytic performance of tailored platinum–tin alloy surfaces for carbon monoxide oxidation

pp 211–220

Céline Dupont, Yvette Jugnet, Françoise Delbecq, David Loffreda*

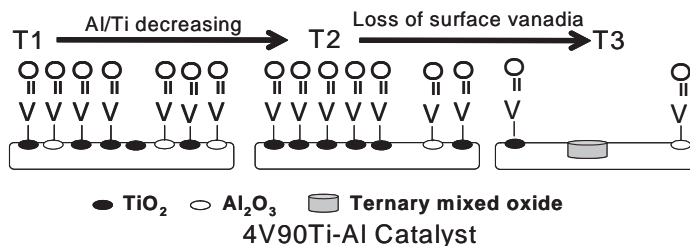


From combined experimental and theoretical approaches, we demonstrate the outstanding capacity of the Pt₃Sn(1 1 1) surfaces for CO oxidation. The mediatory role of tin is elucidated from a charge transfer analysis.

Characterization and reactivity of sol–gel synthesized TiO₂–Al₂O₃ supported vanadium oxide catalysts

pp 221–228

Debaprasad Shee, Goutam Deo*, Andrew M. Hirt

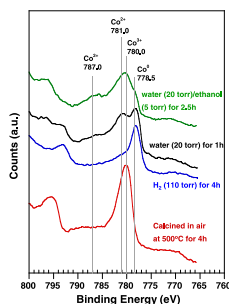


Surface active vanadia species present on TiO₂–Al₂O₃ mixed oxide support depends on loading and calcination temperature. Surface Al/Ti ratio varies with calcination temperature and depends on vanadia loading.

Water-induced formation of cobalt oxides over supported cobalt/ceria–zirconia catalysts under ethanol-steam conditions

pp 229–235

Sean S.-Y. Lin, Do Heui Kim, Mark H. Engelhard, Su Y. Ha*

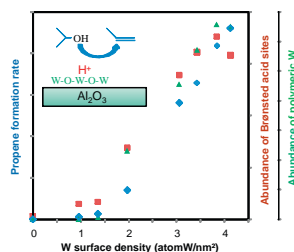


In situ XPS spectra (Co2p region) of the 10% Co/CeO₂–ZrO₂ catalyst as calcined in air at 500 °C for 4 h, and as exposed in different feed conditions at 450 °C.

Correlation between structure, acidity and catalytic performance of WO_x/Al₂O₃ catalysts

pp 236–244

Xueying Chen, Guillaume Clet, Karine Thomas, Marwan Houalla*

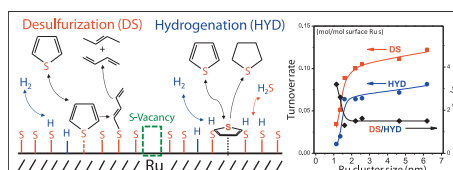


The relationship between the nature of W surface species, acidity and activity, was established for a series of WO_x/Al₂O₃ catalysts. Polymeric W surface species were found to be directly related to the abundance of relatively strong Brønsted acid sites and to the development of the catalytic activity for isopropanol dehydration.

Thiophene hydrodesulfurization catalysis on supported Ru clusters: Mechanism and site requirements for hydrogenation and desulfurization pathways

pp 245–256

Huamin Wang, Enrique Iglesia*

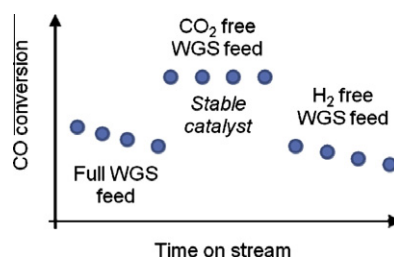


Sulfur vacancies on Ru cluster surfaces bind thiophene and activate H₂ and H₂S in quasi-equilibrated steps that form intermediates involved in kinetically-relevant hydrogenation and H-assisted C–S bond cleavage reactions. Desulfurization and hydrogenation turnover rates increase with cluster size because weaker binding of sulfur atoms on larger Ru metal clusters lead to a larger number of sulfur vacancies during steady-state catalysis.

The effect of reaction conditions on the stability of Au/CeZrO₄ catalysts in the low-temperature water–gas shift reaction

pp 257–265

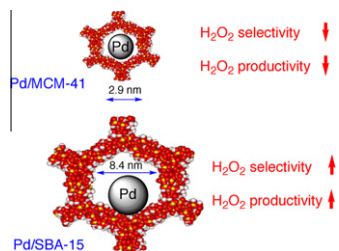
H. Daly, A. Goguet, C. Hardacre*, F.C. Meunier, R. Pilasombat, D. Thompsett



The predominant active state in Au/CeZrO₄ catalysts for low-temperature water gas shift is thought to be Au(0) and, through varying the reaction feed conditions, it was possible to enhance the stability of the catalysts significantly.

Mesoporous silica as supports for Pd-catalyzed H_2O_2 direct synthesis: Effect of the textural properties of the support on the activity and selectivity pp 266–273

Elena Ghedini, Federica Menegazzo, Michela Signoretto, Maela Manzoli, Francesco Pinna, Giorgio Strukul*



SBA-15 allows preparing palladium catalysts with enhanced productivity and selectivity in the direct synthesis of hydrogen peroxide by imparting Pd particles the proper size and distribution.
